

Production of J/ψ vs Multiplicity

In $\sqrt{s} = 510 \text{ GeV } p+p$ Collisions with STAR at RHIC

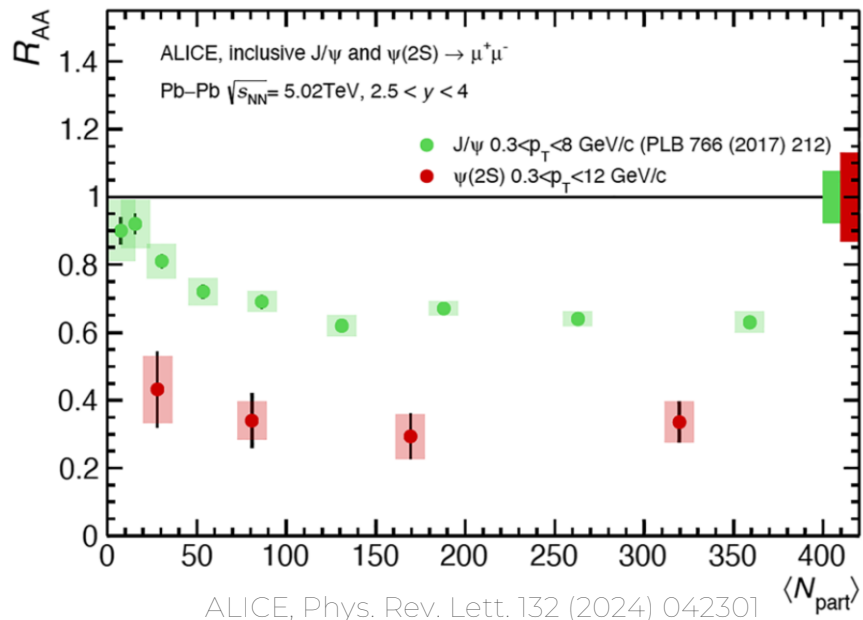
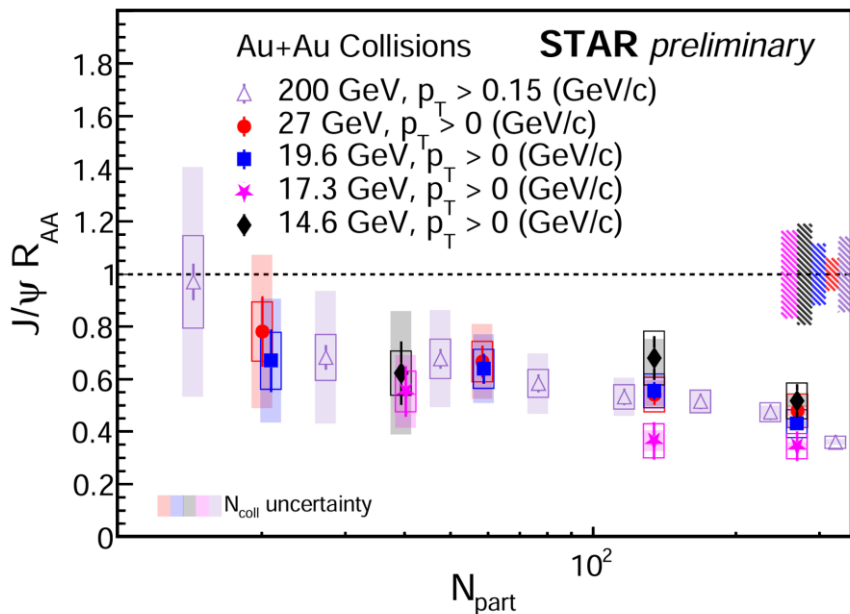
Brennan Schaefer (Lehigh University)
for the STAR Collaboration 24.09.24



Motivation for J/ψ studies

J/ψ was long seen as a golden probe for the presence of the QGP
Suppression of J/ψ is seen more in central than peripheral A+A collisions
Also suppressed in high compared to low multiplicity p+p?

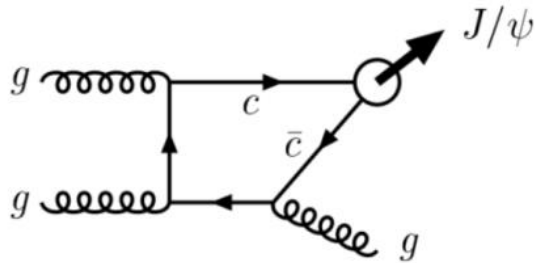
as seen in Wei Zhang's talk tomorrow



Hard Scattering Processes within NRQCD

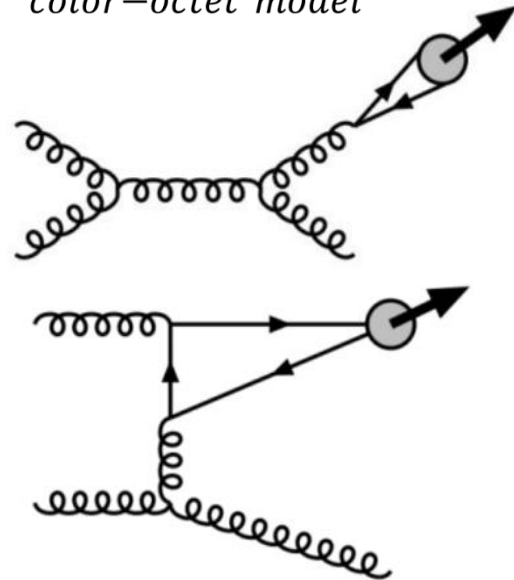
$$d\sigma \sim f(x_1) \otimes f(x_2) \otimes \hat{\sigma}^{x_1+x_2 \rightarrow [c\bar{c}] + X} \otimes H[c\bar{c}] \rightarrow J/\psi$$

color-singlet model



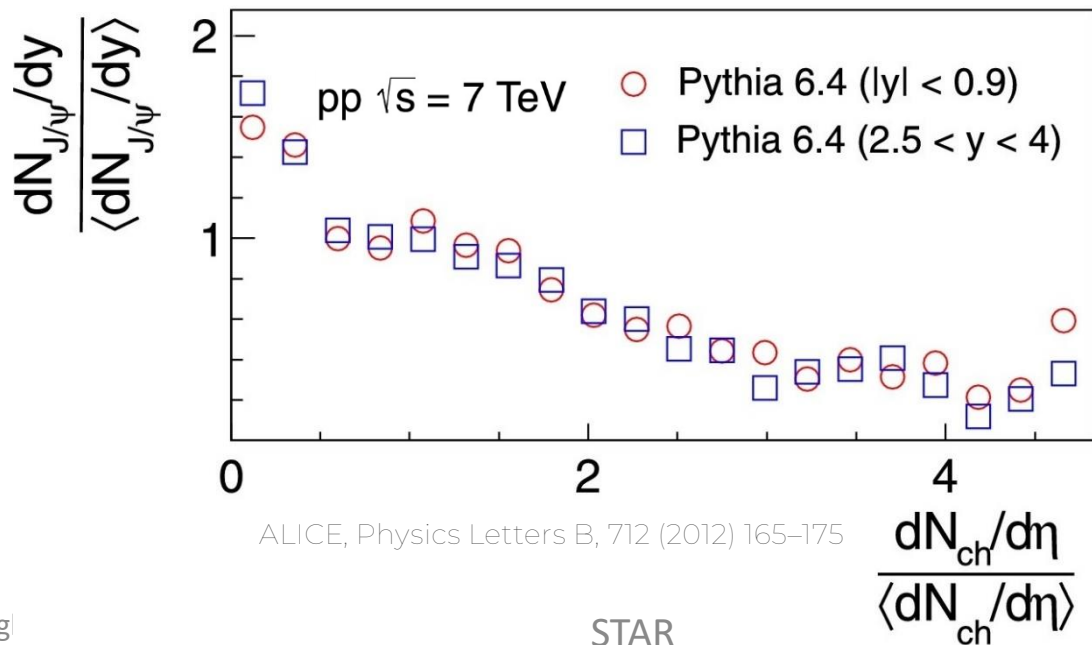
M. Kramer hep-ph/0106120

color-octet model



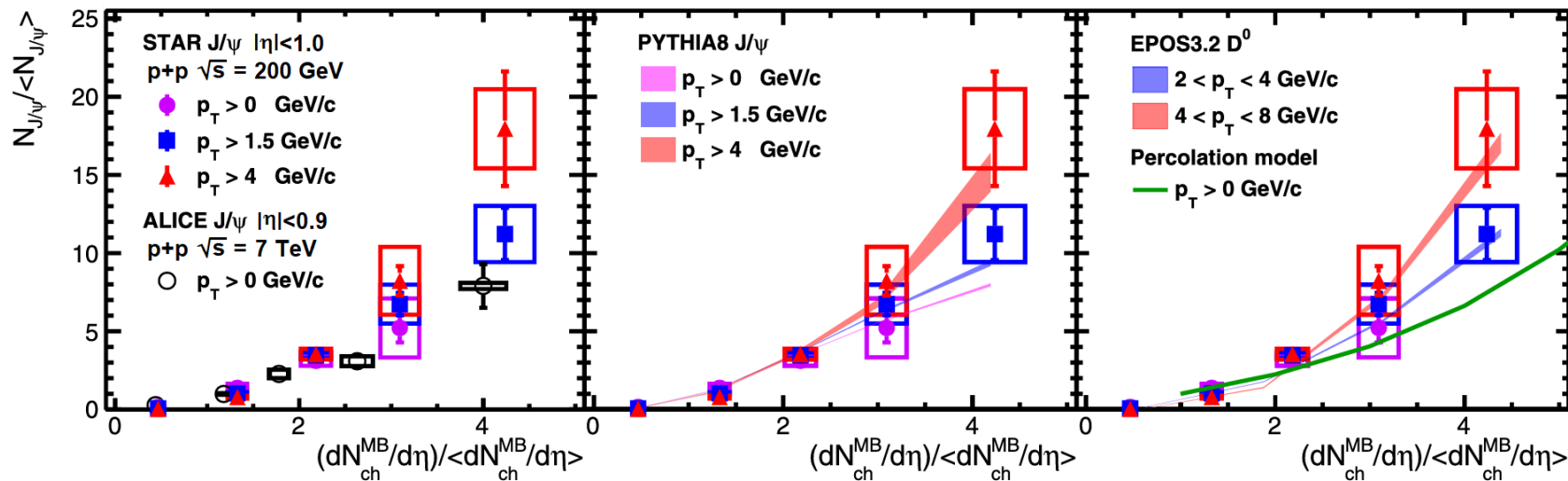
A production baseline

Predictions from NRQCD as implemented in Pythia 6, purposefully involving only hard scattering, and neglecting parton clusters with multi-parton interactions. Even beauty hadron feeddown is absent.



Earlier Measurements

At multiple energies, J/ψ production has been found to rise with respect to event multiplicity, at rates that are faster than linear.

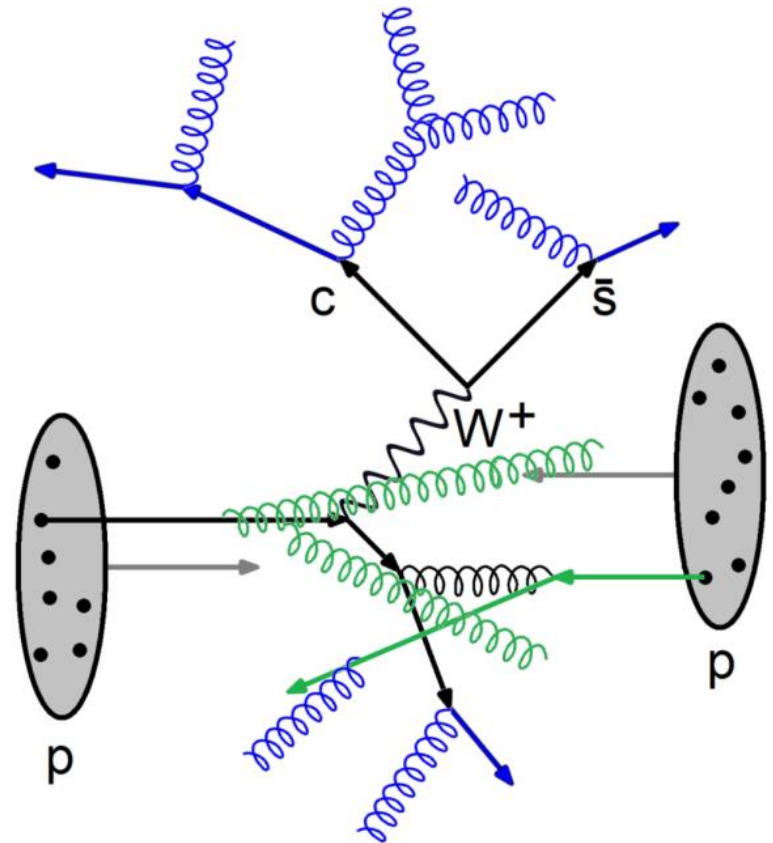


STAR, Physics Letters B 786 (2018) 87–93

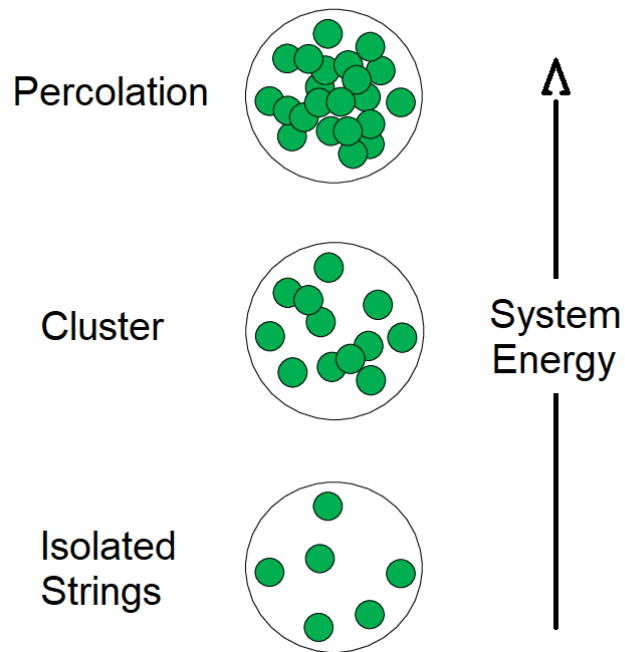
Multi-Parton Interactions

Events that feature more numerous multi-parton interactions are more likely to feature small impact parameters of opposing partons, resulting in enhanced hard scattering processes such as J/ψ production

S. Weber et al. Eur. Phys. J. C (2019) 79:36



Percolation



Percolation of color strings may similarly contribute to the faster than linear increase by diminishing soft hadron production in relation to J/ψ production

E. G. Ferreira, C. Pajares, Phys.Rev.C 86 (2012) 034903

The STAR Detector

Barrel Electromagnetic Calorimeter

0.05 x 0.05 (ϕ x η) towers

$|\eta| < 1.0$

Time of Flight

$r=208\text{cm}$, $\Delta t=100\text{ps}$, $|\eta| < 0.9$

Beam-Beam Counter

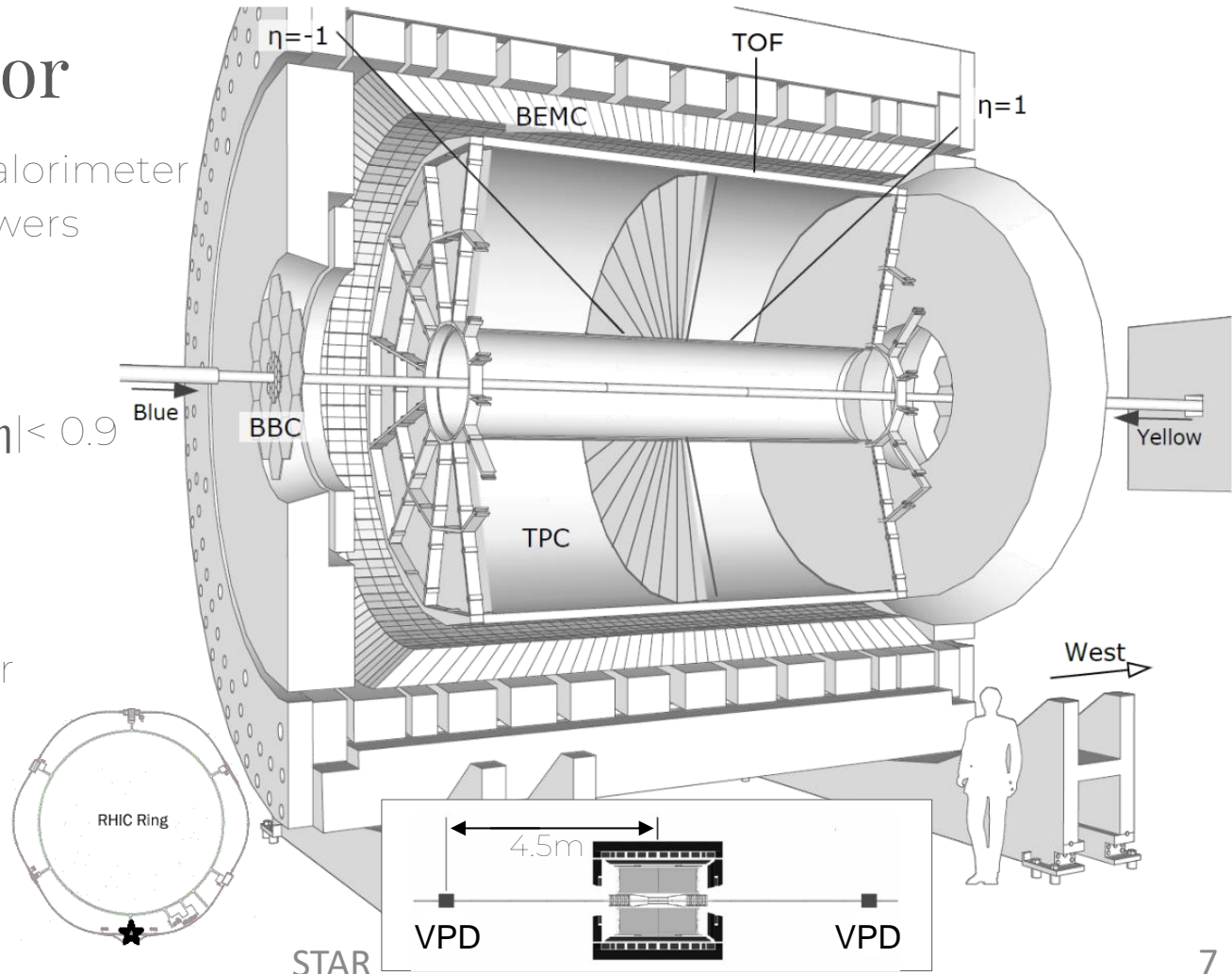
$3.8 < |\eta| < 5.1$

Time Projection Chamber

52.8 m^3 , $|\eta| < 1.0$

Vertex Position Detector

$4.24 < |\eta| < 5.1$



Detector Usage

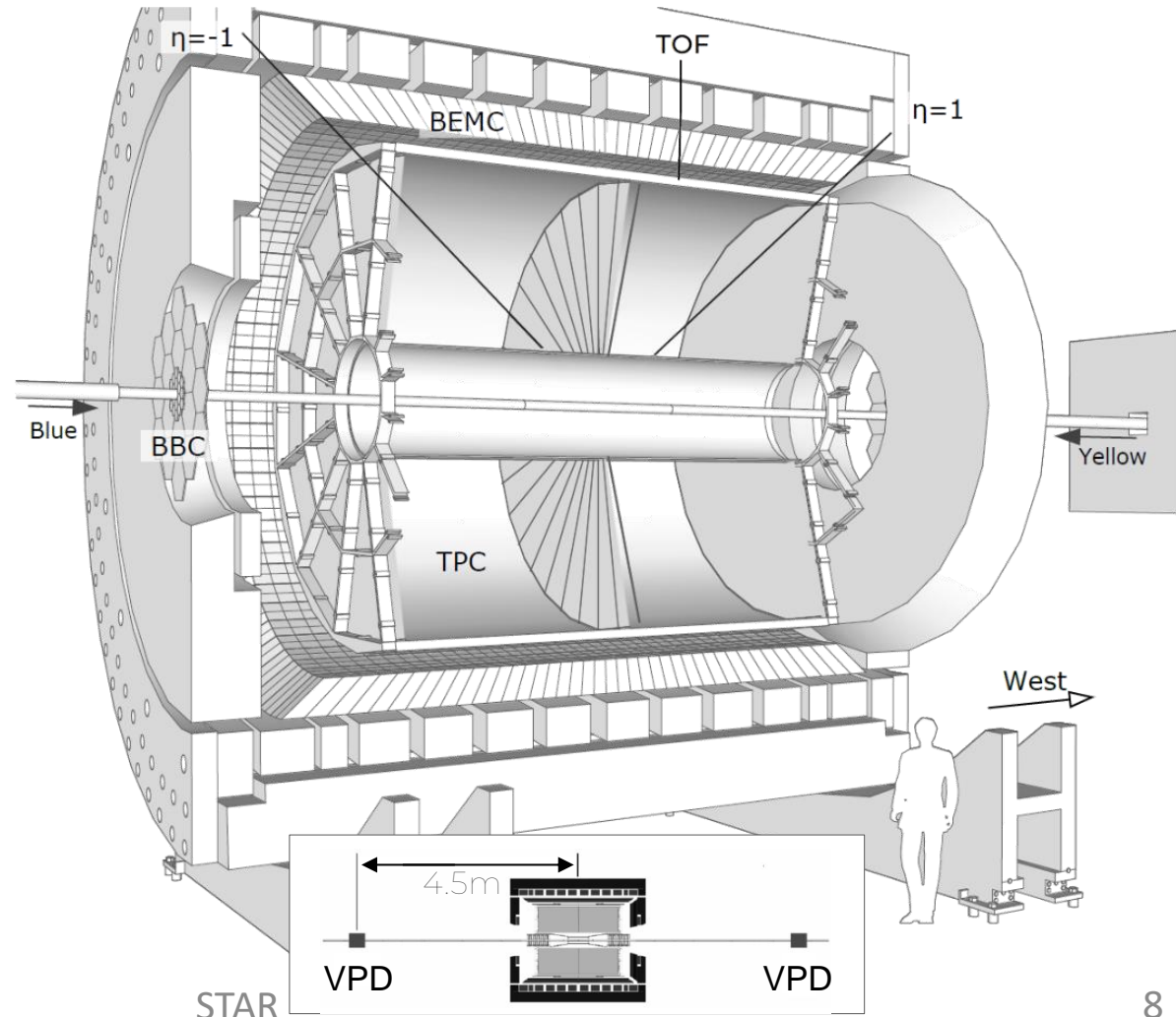
(VPD) Vertex Position Detector
Measure vertex z-position

(BEMC) Barrel EM Calorimeter
Trigger on, identify electrons

(BBC) Beam-Beam Counter
Min-bias trigger

(TPC) Time Projection Chamber
Tracking and dE/dx

(TOF) Time of Flight
Pileup track rejection
Multiplicity estimation
Slow non e^\pm veto



Dataset

2017 STAR $p+p$ at $\sqrt{s} = 510$ GeV
(79.5 pb⁻¹)

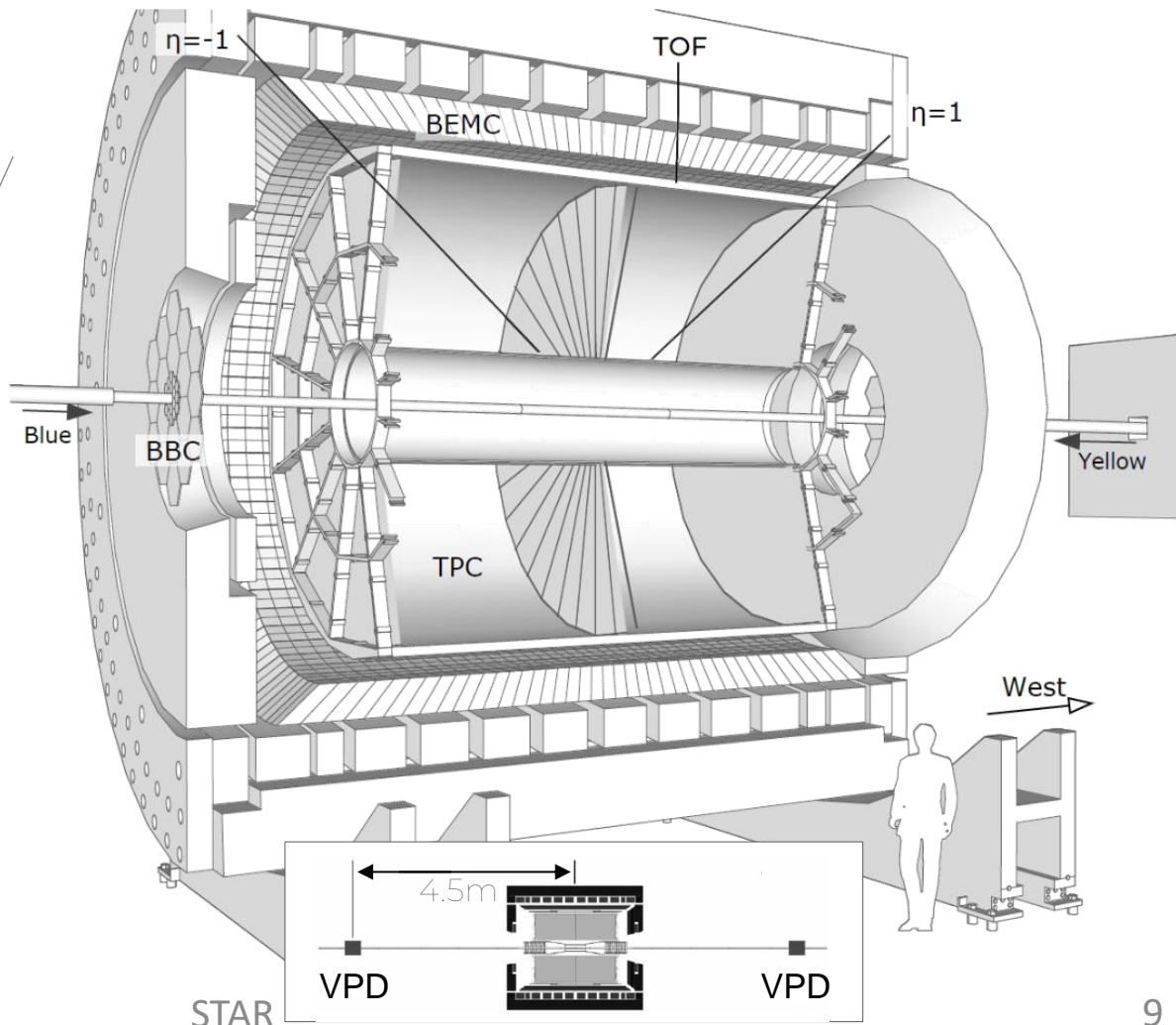
4x increase in luminosity
above J/ψ vs mult. in $p+p$
200 GeV result

Event Selection

Trigger: BEMC Tower with
 $E > 4.2$ GeV

Events in ± 40 cm from $z = 0$

Vertex quality selections



Event Multiplicity

Event activity is characterized using TOF multiplicity: number of tracks matched to TOF hits

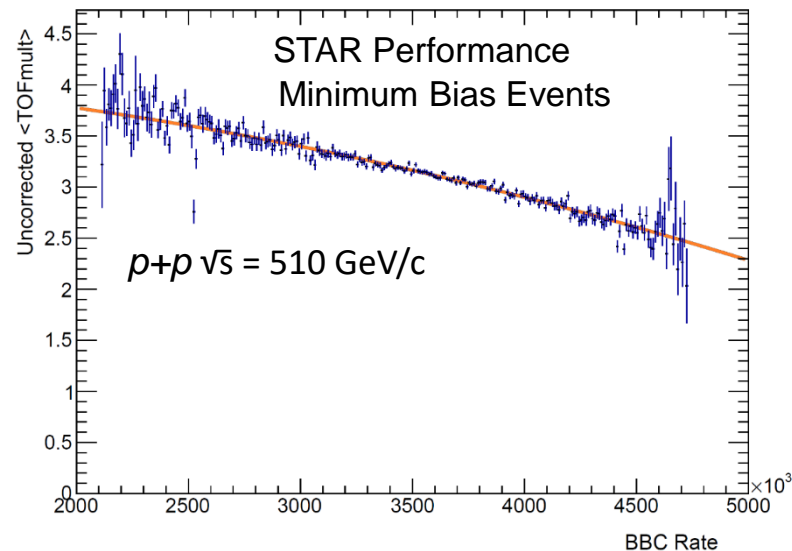
TOF Mult. Track Selection

Track Quality Selections

DCA to PV < 1.5 cm

$|\eta| < 1.0$

Track Matched to TOF Hit



Correction for dependence of tracking efficiencies on occupancy effects accompanying luminosity rate

Correction for trigger efficiencies found from simulation

Decay Product Selection

Track Selection

$$p_T > 0.2 \text{ GeV}/c$$

$$|\eta| < 1.0$$

$$\text{DCA to PV} < 1.5 \text{ cm}$$

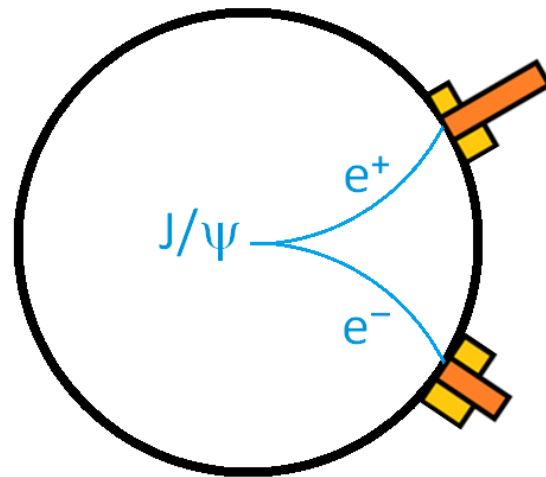
Track Quality Selections

Trigger e^\pm Selection

$$\text{Trigger: } E_{\text{tower}} > 4.2 \text{ GeV}$$

$$dE/dx: -1.9 < n\sigma_e < 3.0$$

$$\text{BEMC: } 2/3 < E_{\text{cluster}}/p < 10/3^*$$



Associate e^\pm Selection

$$\text{Slow non } e^\pm \text{ veto } (0.97 < \beta < 1.03)$$

OR

$$\text{BEMC: } 2/3 < E_{\text{cluster}}/p < 10/3^*$$

*BEMC Clusters: 3 towers

Analysis Procedure

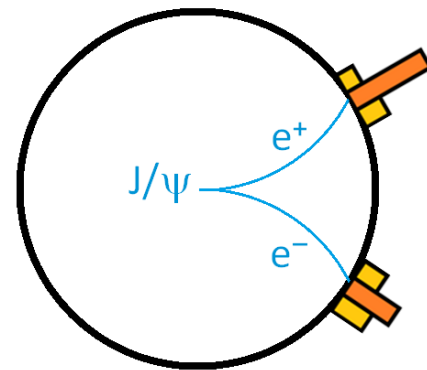
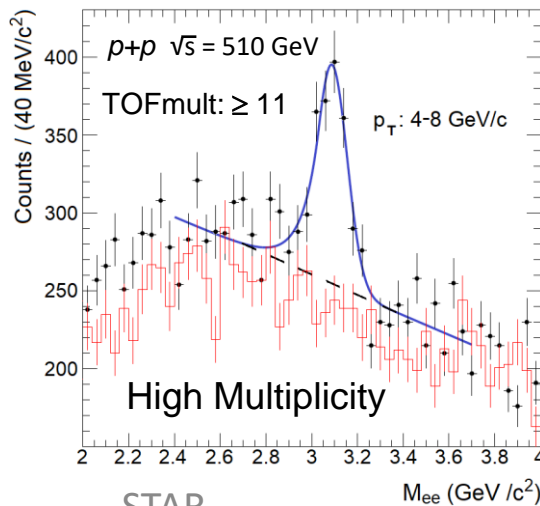
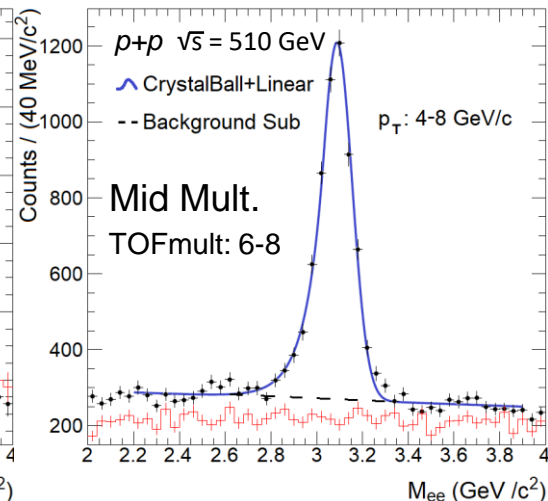
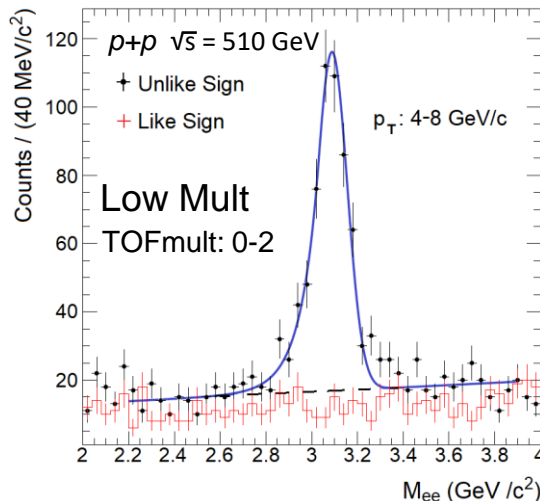
Reconstruct J/ψ in the dielectron channel, using the invariant mass method

Construct unlike-sign invariant mass distribution

Fit distribution with CrystalBall peak + cubic polynomial for background

Centroid of CrystalBall core fixed to PDG world average

Width is variable in fit



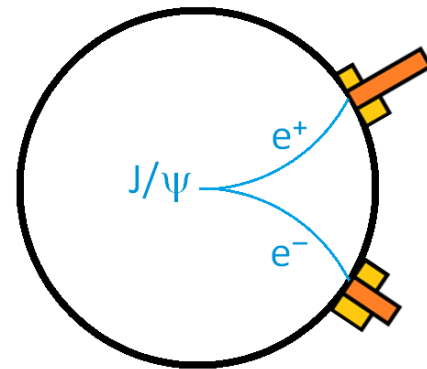
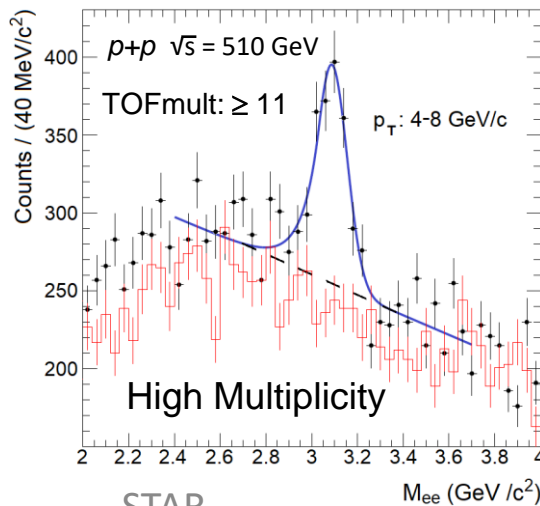
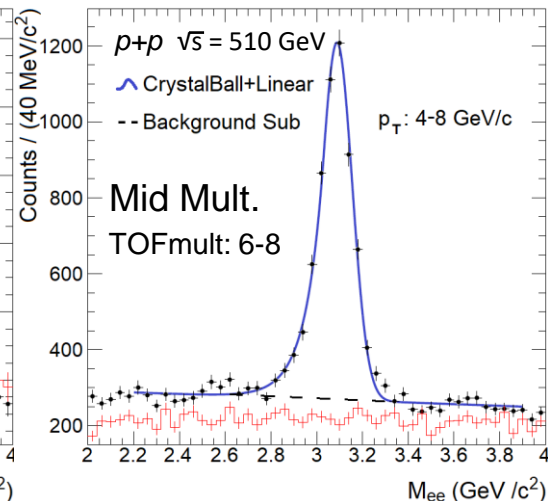
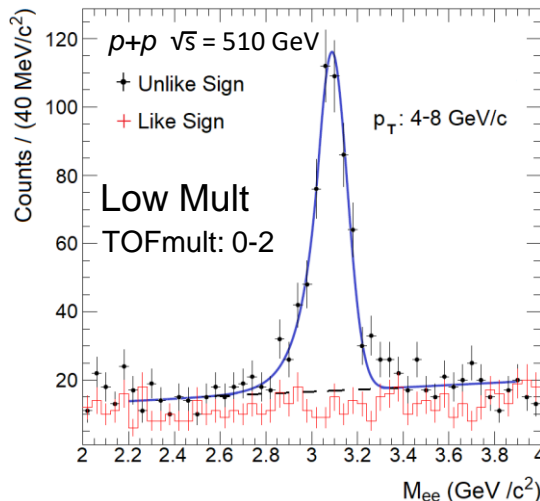
$$M^2 = (E_1 + E_2)^2 - \|\mathbf{p}_1 + \mathbf{p}_2\|^2$$

Yield Extraction

Yield extracted in
 $2.6 < M_{ee} < 3.4 \text{ GeV}/c^2$

Correct for yield beyond this
region

For systematic uncertainties
do both function integration
and histogram integration



$$M^2 = (E_1 + E_2)^2 - \|\mathbf{p}_1 + \mathbf{p}_2\|^2$$

Uncertainties

Systematic Uncertainties				
	Track Quality			1 - 12%
	Daughter Electron Selection			1 - 9%
	Trigger Efficiency Correction			0 - 13%
	Signal & Background			3 - 16%
	Total			3 - 17%
Statistical Uncertainties				3 - 26%

Range of uncertainty variations:
different multiplicity intervals

Results

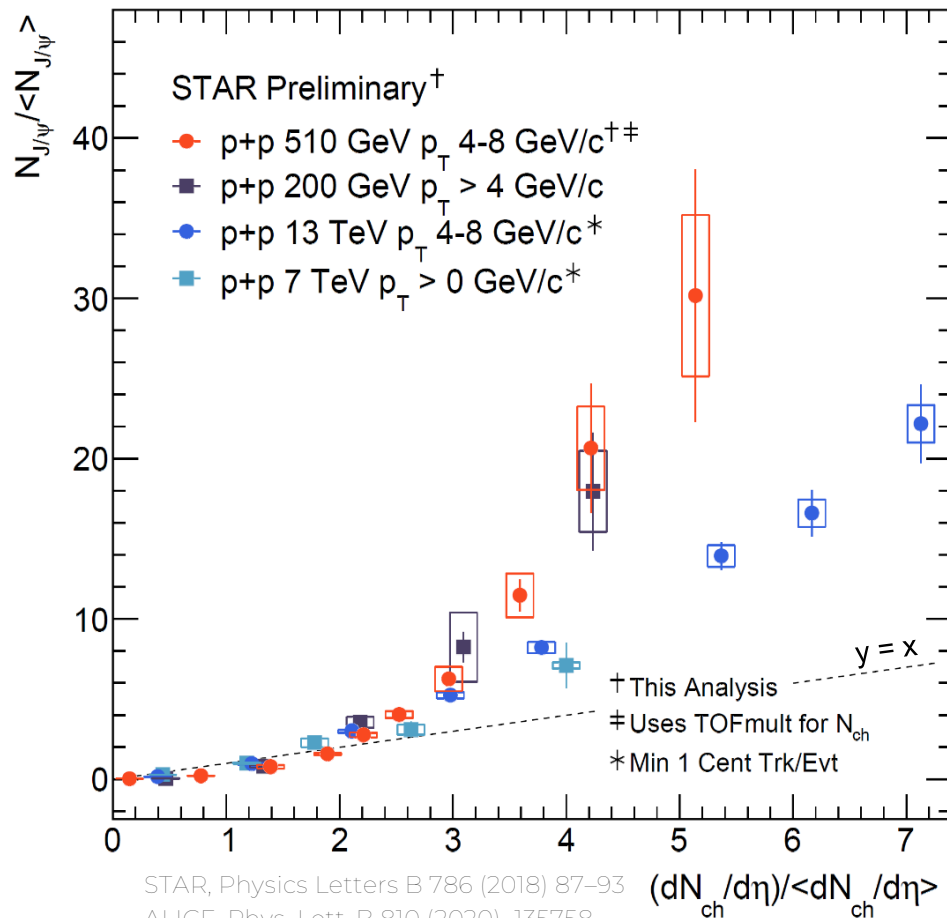
Higher reach in multiplicity than 200 GeV result

Improved multiplicity granularity

Normalized yields at 510 GeV consistent with 200 GeV

200, 510, GeV and 13 Tev results: similar p_T ranges

Hint of splitting between RHIC and LHC energies



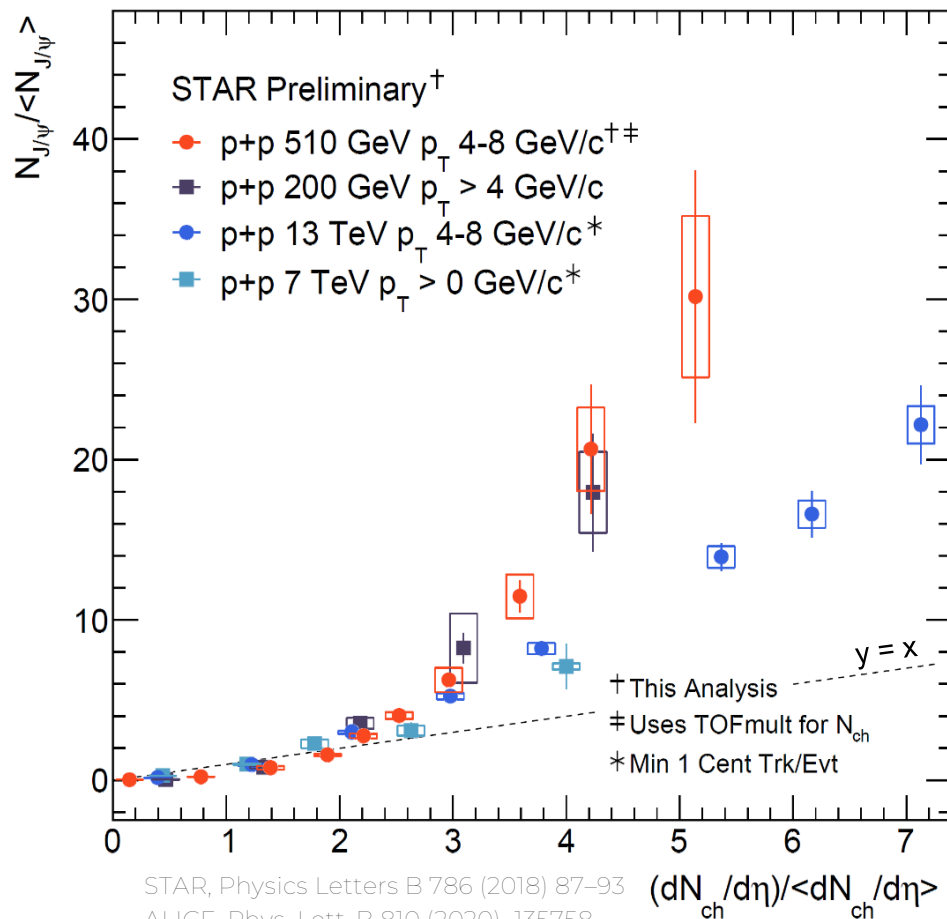
STAR, Physics Letters B 786 (2018) 87–93
 ALICE, Phys. Lett. B 810 (2020) 135758
 ALICE, Physics Letters B, 712 (2012) 165–175

Conclusion and Summary

Unfolding is needed to convert TOF multiplicity into charged particle multiplicity

Comparisons to different models and MC predictions

Parallel study for Υ mesons in progress



STAR, Physics Letters B 786 (2018) 87–93
ALICE, Phys. Lett. B 810 (2020) 135758
ALICE, Physics Letters B, 712 (2012) 165–175

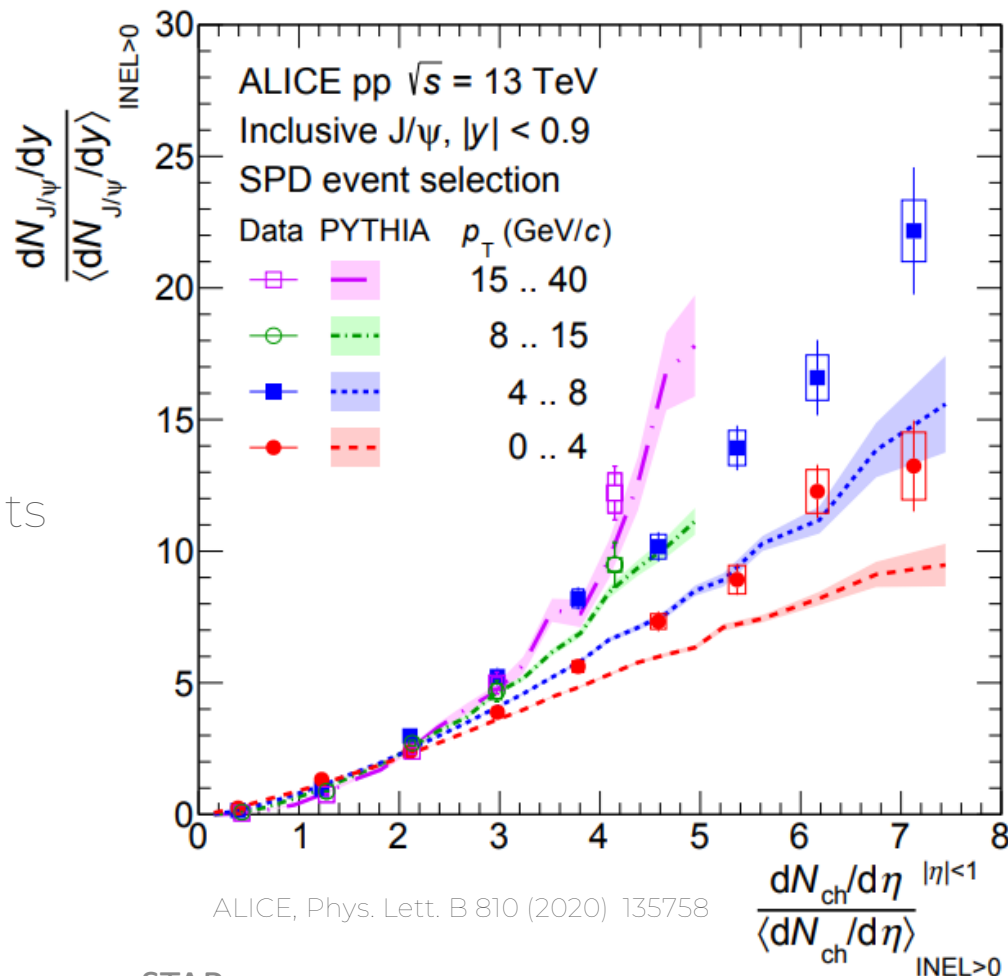
Backup

References

- [1] M. Kramer, Quarkonium Production at high-energy colliders, hep-ph/0106120
- [2] J. Harris, B. Müller, et al, QGP Signatures revisited Eur. Phys. J. C (2024) 84:247
- [3] J. Adam, J/ψ production cross section and its dependence on charged-particle multiplicity in p+p collisions at $\sqrt{s} = 200$ GeV, Physics Letters B 786 (2018) 87–93
- [4] Rubin P, et. al. (CLEO) Observation of the 1P_1 state of charmonium, Phys Rev D, 72 092004, 2005
- [5] B. Abelev et. al. (ALICE) , J/ψ production as a function of charged particle multiplicity in pp collisions at $\sqrt{s} = 7$ TeV, Physics Letters B, 712 (2012) 165–175
- [6] B. Martin, G. Shaw, Nuclear and Particle Physics, 3rd Ed, p. 190
- [7] S. Acharya, et al. (ALICE) Multiplicity dependence of inclusive J/ψ production at $\sqrt{s} = 13$ TeV, Phys. Lett. B 810 (2020) 135758
- [8] S. Weber, et al. Elucidating the multiplicity dependence of J/ψ production in proton-proton collisions with PYTHIA8, Eur. Phys. J. C (2019) 79:36

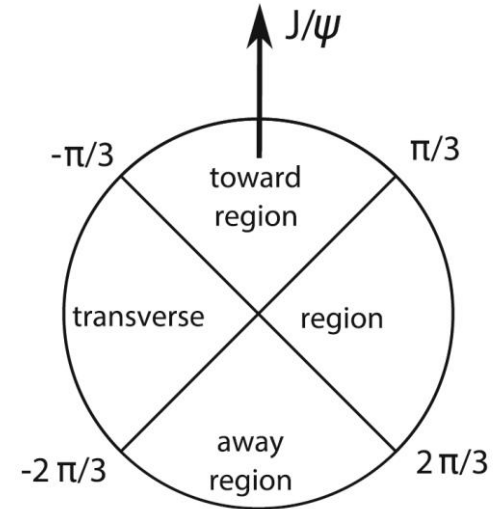
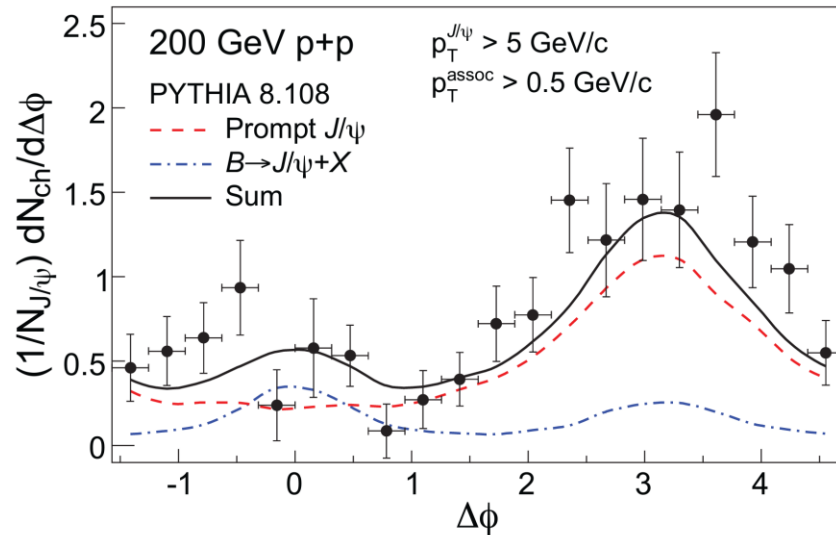
Backup

Model calculations at high multiplicity show qualitative agreement with measurements at LHC energy.



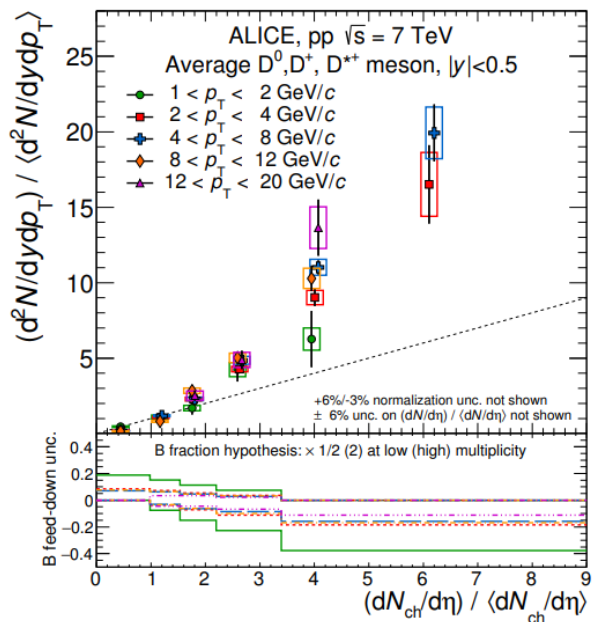
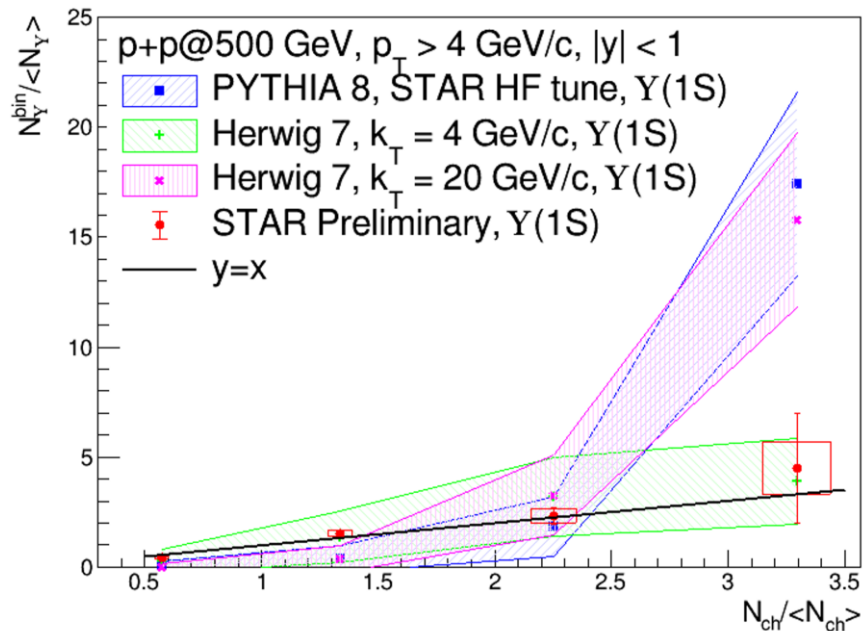
Backup

Model calculations are able to describe the azimuthal distribution with respect to the J/ψ in underlying events



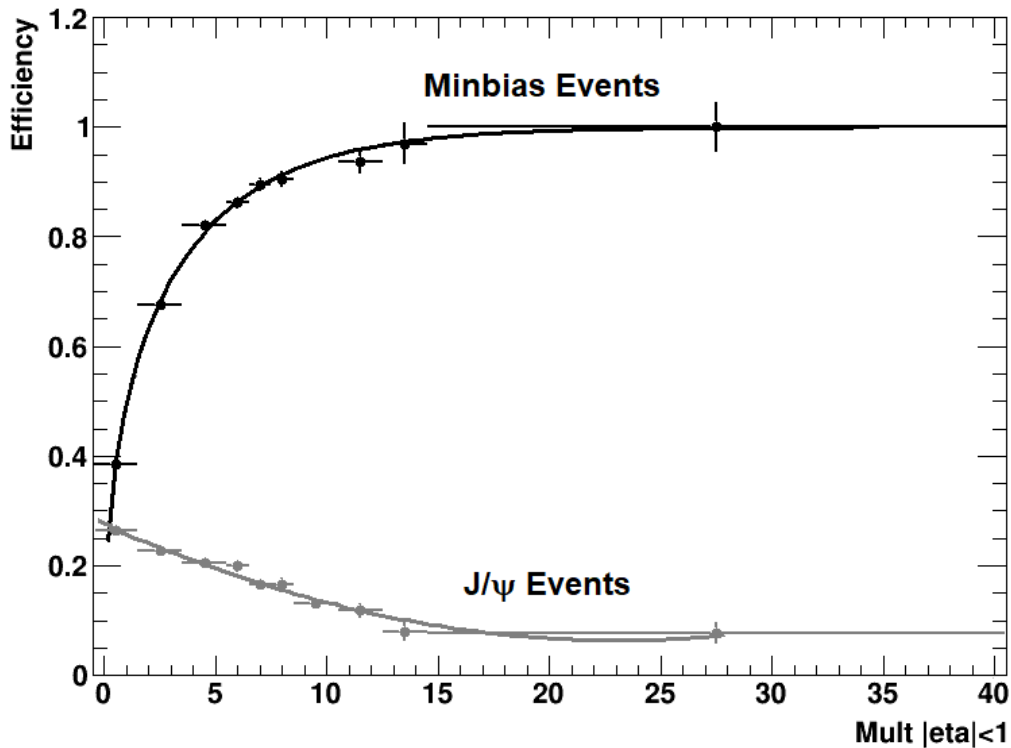
Backup

Comparable event activity dependence featured in production of other open and hidden heavy flavor hadrons



Backup

Separate efficiency vs multiplicity event selection corrections are necessary for the J/ψ and min-bias distributions



Pythia events

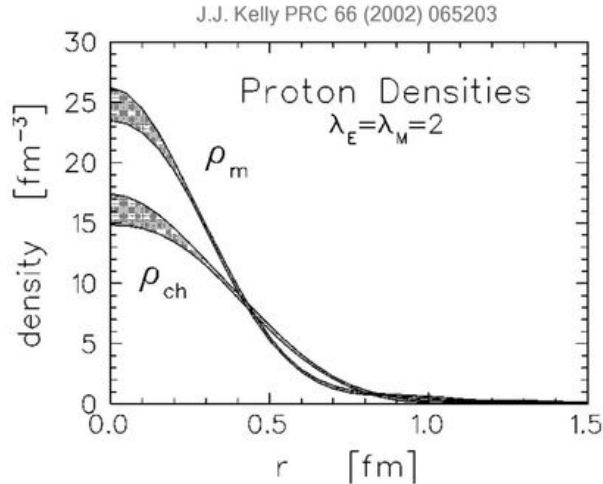
- STAR HF Tune
- MB

embedded into zerobias and reconstructed

Backup

$$F(Q^2) = \frac{G_E^2(Q^2) + \tau G_M^2(Q^2)}{1 + \tau} + 2\tau \tan^2\left(\frac{\theta_e}{2}\right) G_M^2(Q^2)$$

➤ Within a **non-relativistic approach**, electromagnetic **form factors** can be interpreted as the **Fourier transform** of the charge and current **densities** inside the nucleon.



$$\rho_{ch}(r) = \frac{2}{\pi} \int_0^\infty dQ Q^2 j_0(Qr/\sqrt{1+(Q^2/4M^2)}) G_E(Q^2) [1+(Q^2/4M^2)]^{1/2}$$

Dipole behaviour

$$\rho(r) = \frac{\lambda^3}{8\pi} \exp[-\lambda r] \rightarrow F(k) = \int \rho(r) \exp[ik \cdot r] d^3r = \frac{\lambda^4}{(k^2 + \lambda^2)^2}$$

Backup

Further insight into this deviation from linearity can be obtained by investigating the impact parameter dependence of MPI. As mentioned earlier, in PYTHIA the number of MPI per event is related to the matter overlap in the pp collisions and, hence, to the impact parameter b [21]. Figure 3 (left panel) shows the average self-normalized number of MPI per event as a function of the self-normalized b^{-1} . In the most central collisions, the average number of MPI saturates at 3.3 times the mean value. Even higher number of MPI, as

[5]

5.2.1 The strong coupling constant

The strong interaction derives its name from the strong forces acting at distances of order 1 fm that, among other things, bind quarks in hadrons. However, many of the remarkable phenomena discussed in this chapter depend on the fact that the interaction gets weaker at short distances; that is, on asymptotic freedom. Such short-distance interactions are associated with large momentum transfers $|\mathbf{q}|$ between the particles, with

$$|\mathbf{q}| = O(\hbar/r), \quad (5.6)$$

where $r = |\mathbf{r}|$ is the distance at which the interaction occurs. For example, the amplitude (1.47) for scattering from a spherically symmetric potential $V(r)$ becomes

$$\mathcal{M}(q) = 4\pi \int_0^\infty V(r) \left(\frac{\sin(qr)}{qr} \right) r^2 dr \quad (5.7)$$

on integrating over all angular directions. The dominant contributions arise from r values of order q^{-1} as asserted, since for smaller r the integrand is suppressed by the factor r^2 , while for large r it is suppressed by the average over the rapidly oscillating sine factor. Hence in discussing

¹⁰The numerical factor multiplying α_s (i.e. $-4/3$ in this case) depends on the colour state chosen, and we will not discuss it further.

[4]